



Immobilization of biomolecules on cysteamine-modified polyaniline film for highly sensitive biosensing



Qi Cai^{a,c}, Baojian Xu^a, Lin Ye^{b,c}, Zengfeng Di^b, Jishen Zhang^a, Qinghui Jin^a, Jianlong Zhao^{a,*}, Jian Xue^d, Xianfeng Chen^{e,**}

^a State Key Laboratory of Transducer Technology, Shanghai Institute of Microsystem and Information Technology, Chinese Academy of Sciences, No. 865, Changning Road, Shanghai 200050, China

^b State Key Laboratory of Functional Materials for Informatics, Shanghai Institute of Microsystem and Information Technology, Chinese Academy of Sciences, No. 865, Changning Road, Shanghai 200050, China

^c University of Chinese Academy of Sciences, No. 19A, Yuquan Road, Beijing 100049, China

^d SGS China Co., Ltd., 4F, Building 3, No. 889, Yishan Road, Shanghai 200233, China

^e School of Electronic Engineering, Bangor University, Bangor LL57 1UT, United Kingdom

ARTICLE INFO

Article history:

Received 8 August 2013

Received in revised form

24 October 2013

Accepted 1 November 2013

Available online 11 November 2013

Keywords:

Cysteamine

Polyaniline film

Quartz crystal microbalance (QCM)

Immobilization efficiency

Biosensing

ABSTRACT

We present a new cysteamine (CS)-modified polyaniline (PANI) film for highly efficient immobilization of biomolecules in biosensing technology. This electrochemically deposited PANI film treated with CS and glutaraldehyde could be employed as an excellent substrate for biomolecules immobilization. The parameters of PANI growth were optimized to obtain suitable surface morphology of films for biomolecules combination with the help of electron and atomic force microscopy. Cyclic voltammetry (CV) was utilized to illustrate the different electrochemical activities of each modified electrode. Due to the existence of sulfhydryl group and amino group in CS, surface modification with CS was proven to reduce oxidized units on PANI film remarkably, as evidenced by both ATR-FTIR and Raman spectroscopy characterizations. Furthermore, bovine serum albumin (BSA) was used as the model protein to investigate the immobilization efficiency of biomolecules on the PANI film, comparative study using quartz crystal microbalance (QCM) showed that BSA immobilized on CS-modified PANI could be increased by at least 20% than that without CS-modified PANI in BSA solution with the concentration of 0.1–1 mg/mL. The CS-modified PANI film would be significant for the immobilization and detection of biomolecules and especially promising in the application of immunosensor for ultrasensitive detection.

© 2013 Elsevier B.V. All rights reserved.

1. Introduction

Polyaniline (PANI) as a conducting polymer has been attracting immense interest in many practical applications ranging from batteries to biosensors, due to its high stability, simplicity of synthesis, low cost and unique electrochemical properties. Especially, in the area of biosensors, PANI has been successfully exploited in many different applications [1–6]. Various methods are available for the synthesis of PANI, and the most widely used techniques are electrochemical and chemical oxidative polymerizations. PANI is widely considered to have the general polymeric structure as shown in Fig. 1a which consists of ‘y’ reduced (benzenoid diamine, Fig. 1b) and ‘1–y’ oxidized (quinoid diamine,

* Corresponding author. Tel.: +86 21 62511070x5801; fax: +86 21 62511070x8714.

** Corresponding author. Tel.: +44 1248 3824801; fax: +44 1248 361429.

E-mail addresses: jlzhao@mail.sim.ac.cn (J. Zhao), x.chen@bangor.ac.uk (X. Chen).

Fig. 1c) repeating units [7]. As immobilization platform for biomolecules, PANI has been extensively modified on the sensitive surfaces of many biosensors, and its high efficiency of immobilization attributes to high density of reduced amine groups on PANI surface which is directly combined with biomolecules.

Meanwhile, quartz crystal microbalance (QCM) is a mass ultra-sensitive piezoelectric immunosensor to detect proteins on its gold electrode surface at nanogram level. For biosensing applications, QCM has been widely used in different detections, such as, antigen [8–10], affinity ligand [11], free radical [12], and gas [13]. Sai et al. reported a procedure for immobilization of IgG antigen on electrochemically synthesized PANI film which was just linked with cross-linker, glutaraldehyde (GLu) [14]. However, due to considerable inert oxidized units existing in traditional PANI films electrochemically deposited, it seems that immobilization efficiency of subsequent biomolecules was limited.

In this study, how to improve immobilization efficiency of biomolecules on PANI film was emphatically taken into consideration. PANI film was electrochemically synthesized firstly and then

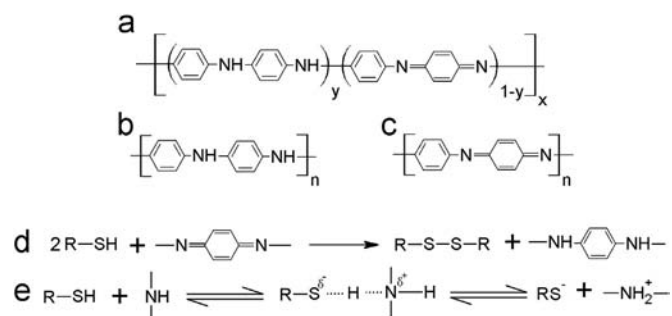


Fig. 1. (a) 2D structures of PANI, (b) reduced unit, (c) oxidized unit, (d) and (e) principles of sulfhydryl reactions with tertiary amine and secondary amine, respectively.

treated with CS and GLu in turn where CS was used to improve the reduction degree of PANI film and the content of reduced amino groups was increased simultaneously. The principle of reaction between CS and PANI was shown in Fig. 1d–e, sulfhydryl group of CS was expected to react with secondary amine and tertiary amine of PANI film, respectively. And, inert tertiary amine could be transformed into active secondary amine (Fig. 1d) and secondary amine could be transformed into more active primary amine (Fig. 1e). Therefore, active amino groups of PANI film were greatly enhanced with CS modification. As cross-linker, GLu has two aldehyde groups: one will covalently combine with these active amino groups on PANI film to form enamine or imine bonds, and the other at the free end will bind amino group in biomolecule. In the present work, field emission scanning electron microscope (FESEM) and atomic force microscope (AFM) were utilized to characterize the surface morphology of PANI film and cyclic voltammetry (CV) was used to illustrate the electrochemical activities of different modified electrodes. Immobilization chemistry of the reactions was investigated in detail with the ATR-FTIR spectroscopy and Raman spectroscopy. As bovine serum albumin (BSA) is a standard protein which has been widely investigated in the field of biomaterials [15–17] and BSA is typically used as blocking protein to reduce the nonspecific binding in immunosensors, it was utilized as the model protein to explore the immobilization efficiency of biomolecules on the optimized PANI film. And comparative experiments with mass changes of BSA immobilization on pure PANI, GLu-linked PANI, CS-modified/GLu-linked PANI, were characterized by a QCM system.

2. Materials and methods

2.1. Materials

All reagents were analytical grade (AR). Aniline, acetone, ethanol absolute and sulfuric acid were purchased from Shanghai Lingfeng Chemical Reagent Co., Ltd. CS and GLu were obtained from Sigma-Aldrich. The bovine serum albumin (BSA) was supplied by Amresco. All solutions such as phosphate-buffered saline (PBS) were prepared by deionized (DI) water (18.2 M Ω cm) obtained from a MilliQ filtration system.

2.2. PANI film deposition method

Gold electrode of QCM was chosen as substrate for PANI deposition, and it was cleaned by sonication for 2 min in acetone and ethanol absolute in turn, rinsed with DI water and dried with blowing nitrogen gas. Before electrochemical deposition, 0.1 M aniline monomer solution should be prepared in 1.0 M sulfuric acid and flushed with nitrogen for 30 min to remove the dissolved

oxygen. And then, PANI film was deposited on the surface of the gold electrode by CV method with EQCM CHI440B. In the three-electrode system, reference electrode (RE) was a KCl-saturated calomel electrode (SCE), and counter electrode (CE) was a platinum wire, and working electrode (WE) was gold electrode of QCM. The potential was scanned from -0.2 to $+0.9$ V at a scan rate of 50 mV/s for growing PANI film. To grow PANI film easier, the potential was firstly equilibrated at 0.1 V versus SCE for 5 s and then positively scanned [18].

2.3. CS modification and BSA immobilization on PANI film

The schematic of CS modification and BSA immobilization on the PANI film of QCM was shown in Fig. 2: (a) PANI-coated QCM chips were washed and sonicated in DI water for 90 s to get smooth and compact PANI film, (b) The fresh PANI film was dipped in 0.1 M CS aqueous solution with stirring for 30 min. (c) After rinsed with DI water and dried with blowing nitrogen gas, CS-modified PANI film was quickly transferred to phosphate buffer saline (PBS, 10 mM, pH=7.4) containing 2.0% GLu for 1 h. (d) After thoroughly washed with PBS and DI water, the film was incubated in BSA solution with different concentration for 1 h, and then rinsed with PBS and DI water twice to wash away nonspecific BSA adsorption. All experiments were carried out at the constant temperature (25 °C).

2.4. Surface morphology characterization

Morphological parameters of the PANI film deposited on gold electrode were characterized by FESEM (Hitachi, S-4800) and AFM (Dimension Icon, Bruker). For AFM, the tapping mode in atmospheric environment with a resonance frequency of 320 kHz, scan rate of 1 Hz/s and resolution of 512×512 pixels was applied.

2.5. Electrochemical measurements

To study the electrochemical properties of the PANI film deposited by electrochemical method, CV-1 was performed in the potential range from -0.2 to $+0.9$ V in aniline free 1.0 M sulfuric acid at a scan rate of 50 mV/s. Moreover, to illustrate the

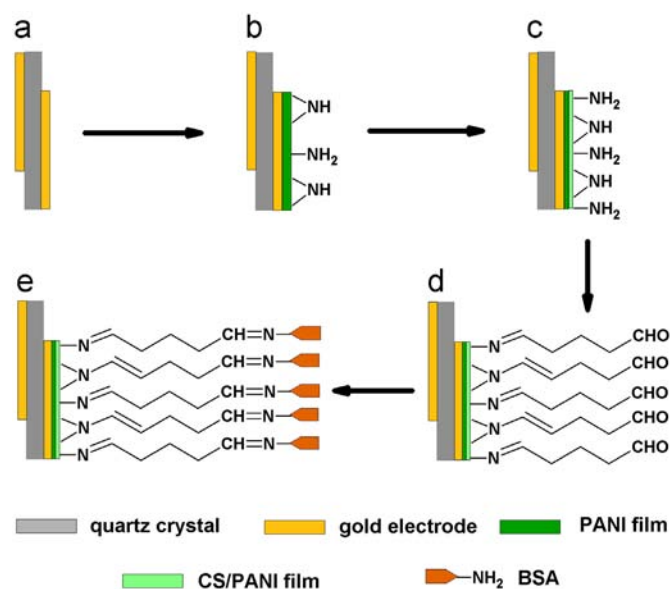


Fig. 2. Schematic of BSA immobilization on PANI films deposited by electrochemical method on gold electrodes of QCM. (a) blank QCM chip, (b) electrochemically deposited PANI film, (c) CS-modified PANI film, (d) CS-modified/GLu-linked PANI film, (e) BSA immobilization on CS-modified/GLu-linked PANI film.

different electrochemical activities of each modified PANI electrode, CV-2 was performed in the potential range from -0.4 to $+0.7$ V in 10 mM PBS (pH 5.8) containing 0.1 M KCl at a scan rate of 50 mV/s.

2.6. ATR-FTIR and Raman characterization

To study the interaction at each step of the process and the changes of chemical groups on the surface of PANI film, surface characterizations were observed by both ATR-FTIR spectroscopy and Raman spectroscopy. ATR-FTIR spectra of pure PANI, CS-modified PANI, only GLU-linked PANI, and CS-modified/GLU-linked PANI, were obtained by Vertex 70 FT-IR Spectrometer, BRUKER, with a scan rate of 128 and a resolution of 4 cm^{-1} . And, the wavenumber range is from 600 to 4000 cm^{-1} . Raman spectra of reduced units and oxidized units of PANI film were recorded with a Raman spectrometer (HORIB Jobin Yvon LabRAM HR800) using a 514-nm laser beam and a charge-coupled detector (CCD) at 4 cm^{-1} resolution. And, the laser power was kept at less 0.1 mW in order to avoid damaging of the samples. Laser beam was focused on the sample with a $\times 100$ objective lens.

2.7. QCM analysis

Immobilization efficiency of BSA protein on the surface of PANI film was taken by QCM analysis. 7.995 MHz, AT-cut, QCM (13.7 mm in diameter) coated with gold in a circular shape (5.1 mm in diameter) on both sides were used for mass-sensitive measurement. And, the resonant frequency of the QCM chip was measured with Electrochemical Quartz Crystal Microbalance (EQCM, CHI440B, CH Instruments., USA). Sauerbry's equation [19] has been established for an AT-cut shear mode QCM to describe the linear relationship between the frequency change (Δf) and the mass change (Δm):

$$\Delta f = -(2f_0^2 / \sqrt{\rho_Q \mu_Q}) \Delta m / A \text{ (in Hz)}$$

where Δf is the measured resonant frequency shift due to the added mass on the surface of the gold electrode; f_0 is the fundamental oscillation frequency of the blank QCM chip, here, $f_0 = 7.995\text{ MHz}$; ρ_Q , the quartz density, has the value of 2.648 g/cm^3 and μ_Q , the shear module, has the value of $2.947 \times 10^{11}\text{ dyne/cm}^2$; A, the area of deposition, is about 0.196 cm^2 in the experiments. Hence, the mass detection limitation of this QCM system is 1.4 ng per Hz. Resonant frequency changes caused by both the deposition of PANI and the immobilization of BSA were emphasized to measure and analyze. It's easy to distinguish BSA immobilization on PANI film at ng level to decide the function of CS treatment for increasing active reduced amino groups in PANI.

3. Results and discussion

3.1. Growth and surface morphology characterization of PANI film

PANI film was electrochemically deposited on surface of gold electrode by using CV method. To standardize the thickness of the film, the number of cycle was kept constant at 10 which gave us a certain thickness in every case of PANI polymerization. And the EQCM system response to the CV method deposition of PANI in 0.1 M aniline and 1.0 M sulfuric acid at a scan rate of 50 mV/s was shown in Fig. 3a and b. Three pairs of specific current peaks [18,20,21], Ox1-Re1, Ox2-Re2, and Ox3-Re3 increased along with increasing cycles (Fig. 3a), and steady PANI growth also resulted in the decrease in frequency with increasing cycles simultaneously (Fig. 3b). In addition, To understand the electrochemical characterization of the PANI film deposited by electrochemical method,

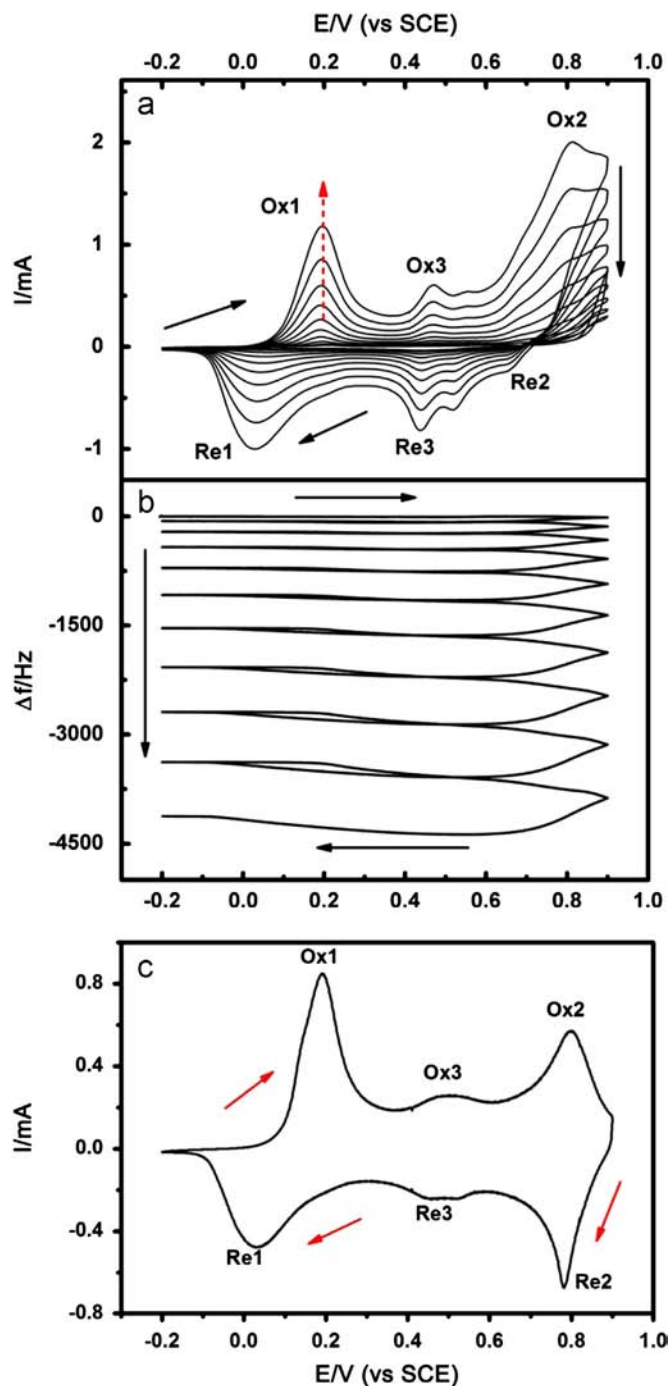


Fig. 3. (a) Current (I) versus potential (E), and (b) frequency change (f) versus potential (E). Curves obtained during CV method in 0.1 M aniline and 1.0 M sulfuric acid at a scan rate of 50 mV/s. (c) Cyclic voltammogram of pure PANI electrode in 1.0 M sulfuric acid with free aniline at a scan rate of 50 mV/s.

CV studies of the above synthesized PANI film were carried out in aniline free 1.0 M sulfuric acid at a scan rate of 50 mV/s [22,23]. The result was shown in Fig. 3c. Three pairs of current peaks Ox1-Re1 (at $+0.19/+0.03$ V), Ox2-Re2 (at $+0.52/+0.49$ V) and Ox3-Re3 (at $+0.80/+0.78$ V) were obtained from the observed voltammogram. Peaks Ox1-Re1 result from the transition between leucoemeraldine and emeraldine, and peaks Ox2-Re2 from the transition between emeraldine and pernigraniline. Peaks Ox3-Re3 may be attributed to the side reactions of the polymer and oligomers of aniline [18].

A prerequisite for uniform and proper covalent immobilization of protein is to have a smooth and compact surface over the region of substrate used for the biosensor [24]. PANI films prepared at different scan cycles (5, 10, 15, and 20) in our experiments showed that the gold electrode on QCM could not be coated fully by PANI film at 5 cycles, the surface morphology of PANI with 10 cycles (Fig. 4a) showed more smooth and uniform surface characteristics than those with 15 (Fig. 4b) and 20 (Fig. 4c) cycles. And the uniformity of the obtained PANI film degraded rapidly with increasing the scan cycles. The stability of subsequent BSA immobilization also proved the PANI film with 10 cycles was more suitable. All the following experiments were conducted with the PANI film deposited by 10 cycles of CV method. To have a further understanding

of the surface morphology and film characterization of the PANI film, SEM and AFM investigations [20,25,26] were carried out, as shown in Fig. 4d–e (FESEM investigation) and Fig. 4f–g (AFM investigation). The data of FESEM with low magnification (Fig. 4d) revealed that there were still polymer particles on the surface of the PANI film though treated with sonication, and the high magnification (Fig. 4e) result showed the deposited film with granule nanostructures. AFM line (Fig. 4f) and region (Fig. 4g) analyses indicated the relief of the PANI film to be in the range of 15–20 nm. Considering the FESEM information and AFM topography, it can be concluded that, the optimized PANI film was electrodeposited as nanogranules and the surface of the gold electrode was adequately distributed to form thin film which was uniform enough to be the final biosensor platform.

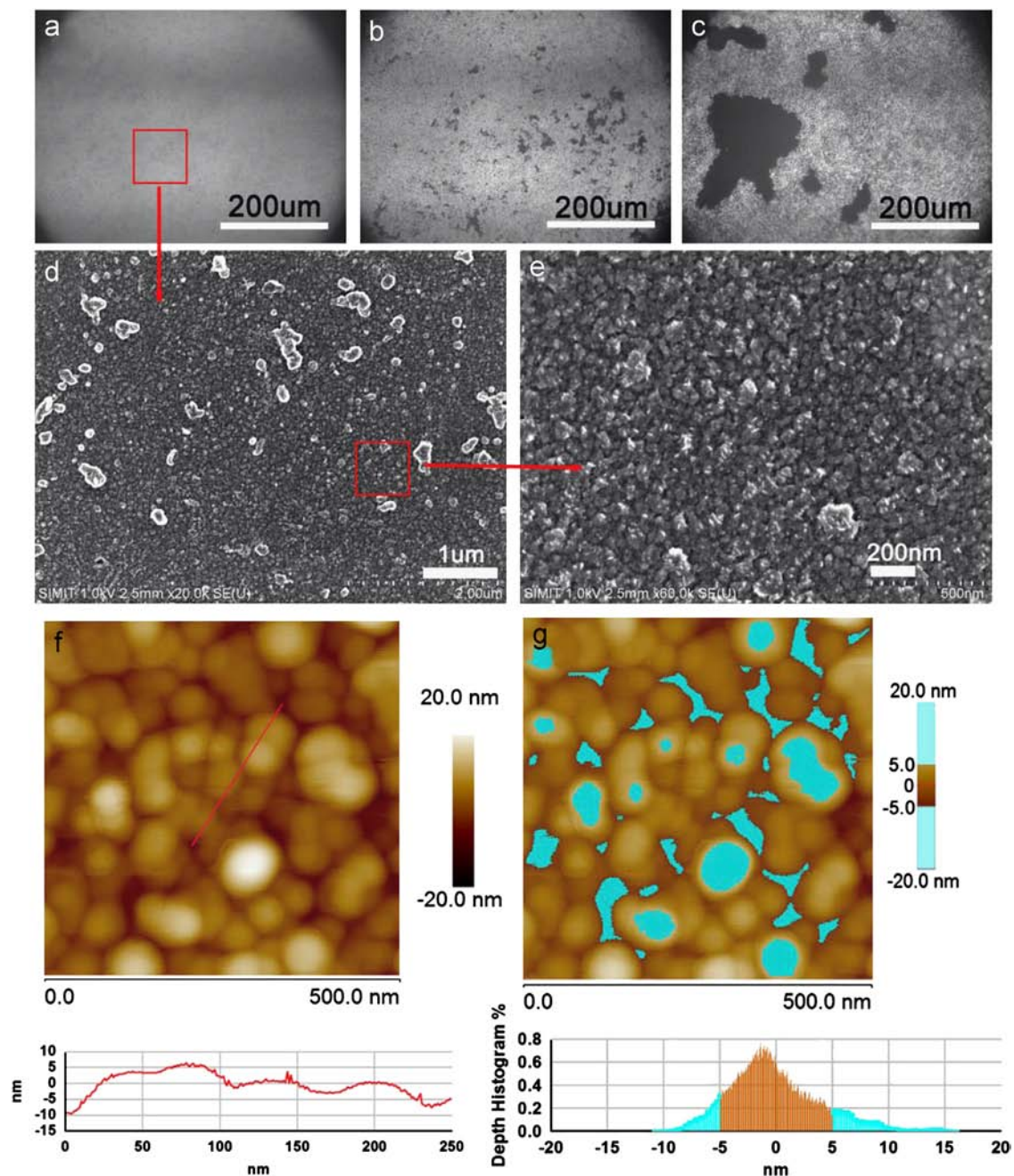


Fig. 4. Morphology of PANI film obtained by CV method with (a) 10 cycles, (b) 15 cycles, (c) 20 cycles of deposition (Images were taken under $\times 40$ magnification). The SEM images (d and e) at different magnifications of PANI film deposited by CV method with 10 cycles. AFM topography of the electrochemical deposited PANI film on gold electrode: line (f) analysis and region (g) analysis to estimate the average height of the deposited PANI film.

3.2. Cyclic voltammograms of different modified electrodes

CV method is a common electrochemical technique used for determining electroactive behavior of materials. In the present study, CV was used to illustrate the different electrochemical activities of (a) pure PANI, (b) CS-modified PANI, (c) CS-modified/GLu-linked PANI, and (d) CS-modified/GLu-linked/BSA PANI electrodes in 10 mM PBS (pH 5.8) containing 0.1 M KCl at a scan rate of 50 mV/s, as depicted in Fig. 5. Generally, PANI remains obvious redox active only in acidic media (pH < 4), however, in slightly acidic media (pH 5.8), the electrochemical activity of PANI declines significantly. Cyclic voltammogram of pure PANI [curve (a)] indicated certain electrochemical behavior at pH 5.8 which was different from the CV curve obtained from 1.0 M sulfuric acid media in Fig. 3c. The pair of broad oxidation/reduction peaks (having positive/negative current values) at +0.40 V/+0.17 V corresponded to the oxidation states of PANI itself. Ping et al. [7] investigated the influence of pH on the CV behaviors of PANI film on Au/Pt electrode. At pH > 4, only one voltammetric response, as a current peak, was obtained and this was consistent with the result in this study. After treated with CS, the color of the PANI film transformed emerald to blue-white (the inset in the lower right corner of Fig. 5), the component of the PANI film was changed and the content of the non-conducting reduced form was increased and the electroactivity of the PANI film was decreased correspondingly and the redox couple shifted about 0.1 V because of the change of component of the CS-modified PANI electrode, which was reflected in the CV response [curve (b)] and supported by the ATR-FTIR analysis results. After addition of GLu, the peak current was further lowered [curve (c)], the covalent reaction between crosslinker and amine groups on the surface of the polymer film might have caused the lowering of peak current. Lastly, peak current of the CS-modified/GLu-linked/BSA PANI electrode encountered a remarkable lowering in magnitude after addition of BSA as shown in curve (d). At this situation, the surface of the PANI film was almost covered by nonconducting BSA molecules and the charge transfer resistance of the modified electrode was increased significantly. Therefore, it might be difficult to achieve electron transfer on the surface of the

modified electrode. These results were consistent with the similar reported data [4,21,26–29].

3.3. Spectrometry results

3.3.1. ATR-FTIR analysis

ATR-FTIR spectra of different chemical states of PANI films were shown in Fig. 6. The typical absorption peaks of pure PANI (Fig. 6a) were observed at 3249, 1589, 1500, 1303, 1159, 1087 and 817 cm^{-1} [30]. The spectra of CS-modified PANI, only GLu-linked PANI, or CS-modified/GLu-linked PANI were found to be similar to pure PANI at the typical peaks as shown in Fig. 6b-d.

The peaks at 1589, 1500, and 1159 cm^{-1} are assigned to the presence of quinoid (Q) structure [30,31], benzene (B) structure [32], and Q structure (a vibration of the $-\text{NH}^+=$ structure formed during protonation) [33,34], respectively. Compared to spectrum of pure PANI, there was no new peak in that of CS-modified PANI film (Fig. 6b). However, it was found that the relative content of 1589 cm^{-1} decreased remarkably and the relative content of 1500 cm^{-1} increased. Furthermore, the relative intensity of the peak at 1159 cm^{-1} decreases significantly. It could be explained that predominant Q structures contained inert tertiary amines in pure PANI were greatly reduced to B structures contained active amines with CS modification. The result consists with the function of CS mentioned above that it can enhance the amount of reduced amino groups on the surface of PANI film.

The peaks obtained at 1754 and 2825 cm^{-1} in Fig. 6c and Fig. 6d could be assigned to the carbonyl (C=O) and C–H stretching of aldehyde groups present on the surface of PANI film, respectively. It was shown that as cross-linker molecules, GLu was immobilized on the surface effectively with covalent binding. However, as the Q and B structure already exist in pure PANI, and the relative concentration of aldehyde groups was very low in GLu-treated PANI film, it might be difficult to have quantitative analysis of the effect of CS and GLu, using ATR-FTIR spectral analysis.

3.3.2. Raman analysis

Raman spectra of different chemical states of PANI films, including pure PANI film synthesized using the CV method,

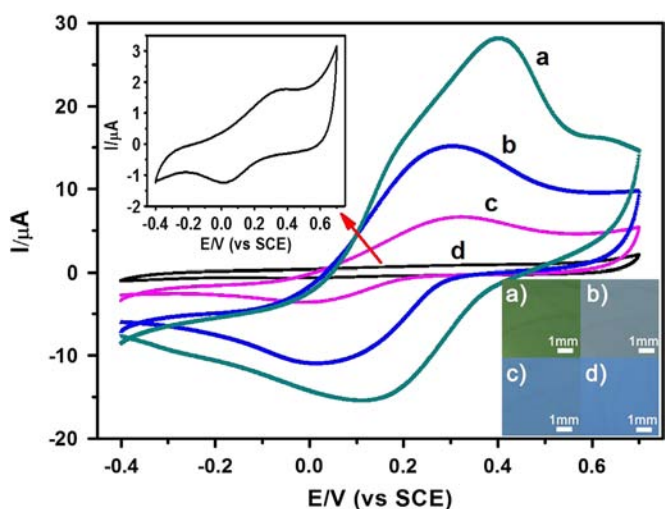


Fig. 5. Cyclic voltammograms of (a) pure PANI, (b) CS-modified PANI, (c) CS-modified/GLu-linked PANI, and (d) CS-modified/GLu-linked/BSA PANI electrodes in 10 mM phosphate-buffered saline (pH 5.8) containing 0.1 M KCl at a scan rate of 50 mV/s. The inset in the top left corner was the amplified CV curve of CS-modified/GLu-linked/BSA PANI electrode and the inset in the lower right corner was the colors of different modified PANI electrodes, respectively. (For interpretation of the references to color in this figure legend, the reader is referred to the web version of this article.)

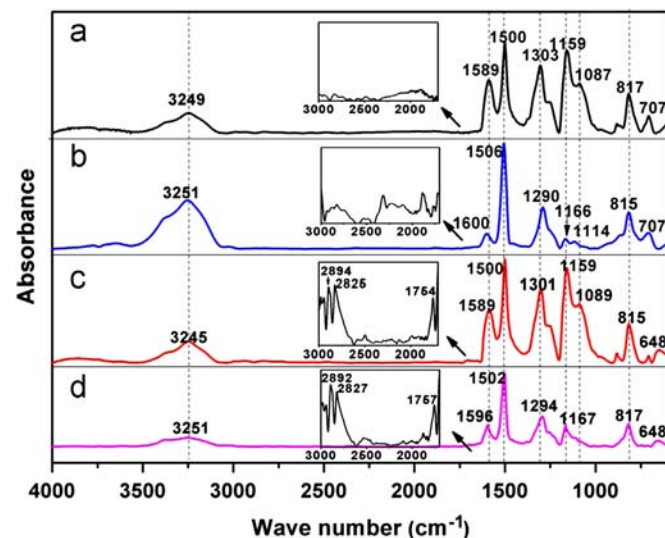


Fig. 6. ATR-FTIR spectra of (a) pure PANI, (b) CS-modified PANI, (c) only GLu-linked PANI, and (d) CS-modified/GLu-linked PANI. The assignment of typical absorption peaks were as follows: 3249 cm^{-1} , NH_2 and NH ; 1589 cm^{-1} , quinoid (Q) structure; 1500 cm^{-1} , benzene (B) structure; 1303 cm^{-1} , C–N of QBQ, BBQ and QBB; 1159 cm^{-1} , C–H in plain vibration; 817 cm^{-1} , C–H out of plain vibration.

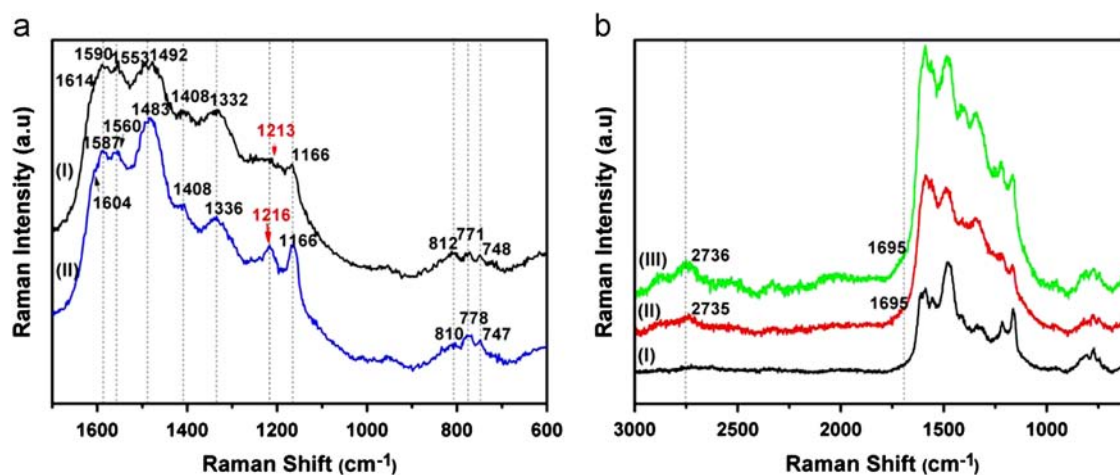


Fig. 7. (a) Raman spectra of (I) pure PANI and (II) CS-modified PANI. (b) Raman spectra of (I) pure PANI, (II) only GLU-linked PANI, and (III) CS-modified/GLU-linked PANI. The assignment of typical Raman bands of PANI were as follows: 1614 cm^{-1} , C–C of benzene (B); 1590 cm^{-1} , C=C of quinoid (Q); 1553 cm^{-1} , C–C of B; 1492 cm^{-1} , C=N of Q; 1408 cm^{-1} , C–C of Q; 1332 cm^{-1} , C~N⁺ in polaronic units; 1213 cm^{-1} , C–N of B; 1166 cm^{-1} , C–H bending of Q; 1695 cm^{-1} , C=O of aldehyde group; 2736 cm^{-1} , C–H of aldehyde group.

CS-modified PANI, only GLU-linked PANI, and CS-modified/GLU-linked PANI in turn, were displayed in Fig. 7. Specific Raman spectra of PANI were described as (1) 1100–1210 cm^{-1} region, where C–H bending vibrations of benzene or quinone type rings are most prominent, (2) 1210–1520 cm^{-1} region with characteristic C–N, C=N and C~N⁺ (where '~' denotes an intermediate bond between a single and a double) stretching vibrations, (3) 1520–1650 cm^{-1} region with the dominating C–C and C=C stretching vibration of benzene and quinone type rings, respectively [35,36]. In addition, the bands below 1100 cm^{-1} , such as the band near 820 cm^{-1} could be assigned to the amine deformation of B, the band near 780 and 750 cm^{-1} could be assigned to the ring deformation and imine deformation of Q structure respectively.

In order to investigate the effect of CS modification on the surface of PANI film, the comparative result on bare PANI and CS-modified PANI was shown in Fig. 7a. Curve I of Fig. 7a showed the typical Raman bands of PANI such as 1614, 1590, 1553, 1492, 1408, 1213 cm^{-1} , 1166, ~780 and ~750 cm^{-1} were totally recorded. Compared to Raman spectrum of pure PANI, there was no new band in the Raman spectrum of CS-treated PANI in curve II of Fig. 7a, but significant change at ~1213 cm^{-1} was recorded. The band at ~1213 cm^{-1} could be assigned to the C–N bending of B structure [37,38]. It should be concluded that CS-modified PANI surface generated more B structure contained active amine and the result consisted again with the function of CS mentioned above. In addition, compared to curve I (pure PANI) of Fig. 7b, the bands emerging at 2736 and 1695 cm^{-1} in both curve II (only GLU-linked PANI) and III (CS-modified/GLU-linked PANI) of Fig. 7b could be assigned to C–H and carbonyl (C=O) stretching of aldehyde groups present in a low concentration on the surface of PANI film [39]. Furthermore, comparative study between curve II and III showed these two peaks with CS-modified PANI were increased much higher than those without CS-modified one, that is, more active aldehyde groups on CS-modified PANI were generated for the linking process of biomolecule immobilization. As well as ATR-FTIR spectral analysis, Raman analysis could provide powerful evidences for CS function in PANI surface modification, while both two analyses could not give quantitative data to explain the effect of CS.

3.4. QCM quantitative results

PANI was deposited onto gold electrodes of quartz crystals as described in Section 2.2. BSA was immobilized following the

optimized protocol. After analysis the surface characterization of different chemical states of PANI film, the ability of protein immobilization of PANI film was measured using QCM system. Since the stability of QCM is a key factor to influence the detection accuracy [6], the QCM was placed in a thermostatic shielded chamber at 25 °C to prevent the frequency stability from affecting by ambient temperature fluctuations and all the measurement equipments were started for 20 min in advance so as to make the equipments stable enough. The result showed that the AT-cut model of QCM was of excellent accuracy with ± 1 Hz in 2 h at 25 °C, and the results were highly reproducible.

In order to investigate the effect of BSA physical adsorption on PANI, blank control-I of pure PANI film without any modification was designed to immobilize BSA. Meanwhile, in order to make clear the effect of CS modification on PANI, control-II of only GLU-linked PANI film was designed. Comparative results obtained from control-I and control-II could help us to understand the difference between physical adsorption and covalent chemical binding, and comparative results from control-II and CS-modified/GLU-linked PANI could find the real effect of CS to PANI film for immobilization of biomolecules. Frequency changes caused by above three kinds of PANI film in different concentrations of BSA were shown in Fig. 8. After three films were incubated in gradient concentrations (from 0.1 to 1 mg/mL) of BSA solution, the frequency changes were recorded using the QCM system mentioned above. Comparing the immobilization results between control-I and control-II, it is clear that the amount immobilization of protein by covalent immobilization was significantly higher than that of the physical adsorption (Fig. 8a), which was consistent with the reported result [12].

Furthermore, QCM frequency results from BSA immobilization on only GLU-linked PANI and CS-modified/GLU-linked PANI proved that CS could be used to improve immobilization efficiency significantly in the certain BSA concentration range from 0.1 $\mu\text{g/mL}$ to 1 mg/mL (Fig. 8a). In this study, the increment of immobilization efficiency was defined as $\eta = |\Delta f_2 - \Delta f_1| / \Delta f_1 \times 100\%$, where Δf_1 and Δf_2 were the frequency changes obtained from BSA immobilization on only GLU-linked PANI and CS-modified/GLU-linked PANI, respectively. As shown in Fig. 8b, BSA immobilization of CS-modified/GLU-linked PANI was higher than that of only GLU-linked PANI, and the immobilization efficiency could achieve an increase of at least 20% in the certain BSA concentration range from 0.1 $\mu\text{g/mL}$ to 1 mg/mL. Especially, maximum increase was about 80% at BSA concentration of 0.1 $\mu\text{g/mL}$. Moreover, it was found that the

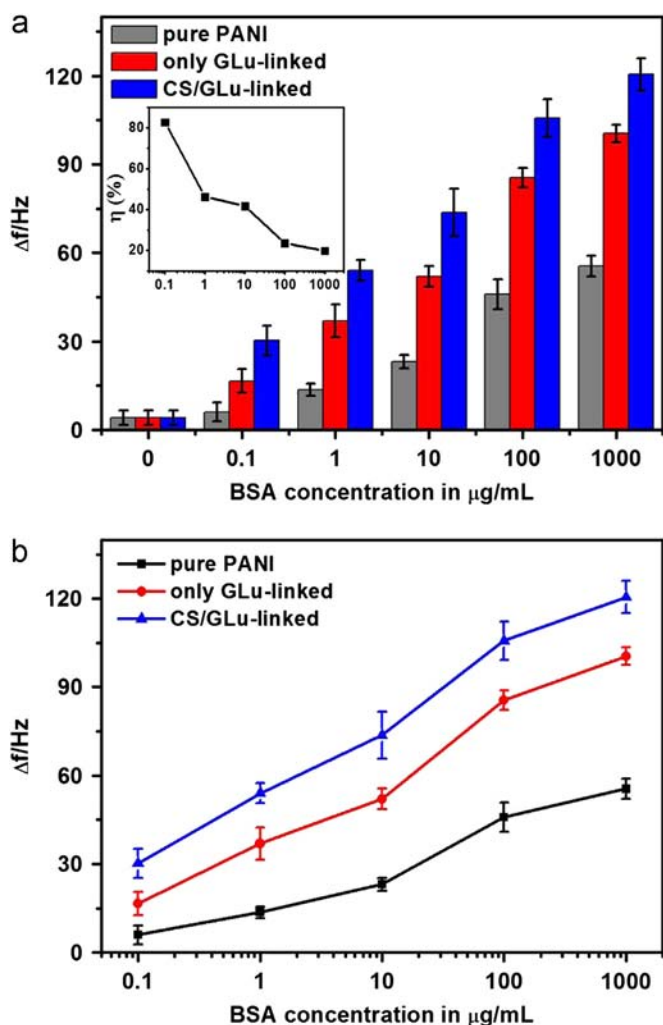


Fig. 8. Comparative experiments on frequency changes of QCM with three kinds of PANI films after immobilization of different concentrations of BSA respectively. (a) Column chart, (b) logarithmic chart. Three kinds of PANI films refer to pure PANI for physical adsorption, only GLu-linked PANI, and CS-modified/GLu-linked PANI.

increment of immobilization efficiency decreased along with the increase of BSA concentration (inset in Fig. 8a) due to the saturated covalent absorption and the increasing physical absorption on PANI film. Specifically, in high BSA concentration, almost all of active amine groups on the surface of both CS-modified/GLu-linked PANI and GLu-linked PANI film were covalently immobilized BSA molecule entirely, and the physical adsorption of BSA increased significantly and dominated the frequency change to reach a stable value. Therefore, CS-modified PANI film for BSA immobilization on the surface of biosensor was effective and sensitive to BSA solution with the concentration range from 0 to 1 mg/mL.

At this point it is necessary to compare methodology and efficiency of our system with the current literature available on biomolecules immobilization based on PANI film. Various methods for immobilizing biomolecules have been reported in the literature such as physical adsorption, entrapment, covalent binding, and LB films. Among all the methods, covalent binding is the most preferred method of immobilization because of its simplicity and stability. For the PANI film herein, electrochemical entrapment and covalent binding were reported to immobilize the biomolecules such as antibodies and enzymes. Grennan et al. [24] and Mathebe et al. [40] immobilized the enzymes on the PANI film using electrochemical entrapment. And Borole et al. [41] immobilized the glucose oxidase (GOD) through potentiodynamic scanning.

Although these methods were simple, the stability and repeatability were not ideal. Moreover, Sai et al. [14] immobilized the antibody on the PANI film by covalent binding with the help of cross-linker GLu and this method was more stable, which provides guidance for our work. In this study, the electrochemically synthesized PANI film was only treated with CS to improve the immobilization efficiency of biomolecules. And from the QCM analysis results, it can be concluded that CS has significant effect on immobilization of biomolecules with low concentration which suggests the promising application of CS-modified PANI film on detection of biomolecules with low density in the further work.

Furthermore, in order to illustrate the feasibility in biosensor application, the improved method was preliminarily used to detect the carcinoembryonic antigen (CEA), which is a tumor mark in early diagnosis of lung cancer. And the immobilization protocol was as following: after the optimized PANI film was treated with CS and GLu in turn, the Anti-h CEA 5909 antibodies were immobilized on the PANI film to determine the specific binding of CEA antigens, and BSA was used as the blocking protein to reduce the nonspecific binding (NSA) of proteins to the immobilized surface. Then the antibody (Anti-h CEA 5909)-modified QCMs were incubated in 10 μg/mL CEA and the frequencies of before and after antigen CEA immobilization were measured. In the control group, Anti-h CEA 5909 was directly immobilized on the PANI film without CS treatment. The frequency change of the experimental group was 30.2 ± 5.8 Hz and the control group was 19.3 ± 4.5 Hz and the corresponding increment of immobilization efficiency η was about 50%, which was consistent with the BSA analysis results. Herein, the usage of CEA detection was only utilized to prove the effectiveness of the new method for biomolecules immobilization and feasible application in biosensors. The specificity and sensitivity of this detection would be taken into consideration in the further work.

4. Conclusion

In this report, we have described a new method to improve the immobilization efficiency of biomolecules on the surface of PANI film, which has been utilized in many biosensors. With the help of CV method, the different electrochemical activities of each modified electrode were illustrated. And from the results of ATR-FTIR and Raman spectroscopy, it was proved that CS could react with PANI film deposited by CV method and the content of reduced amino group was enhanced. In addition, with QCM sensor, it was found that the amount of BSA immobilization could be improved on CS-modified/GLu-linked PANI compared to on only GLu-linked PANI. CS modification on PANI would be significant for the immobilization and detection of biomolecules. Furthermore, since the CS-modified PANI film forms an excellent and high efficiency thin layer for the immobilization of biomolecules, this technology may be promising to use in other biosensors needed immobilizing biomolecules such as piezoelectric immunosensors or SPR biosensors.

Acknowledgement

This work was supported by Grants from the National Basic Research Program of China (973Program) (No.2012CB933303, No.2011CB707505), the National Key Technology R&D Program (No.2012BAK08B05), Science and Technology Commission of Shanghai Municipality (Grant No.11ZR1443900, 11391901900, 11530700800, 10391901600), the National Science Foundation of China (No. 21275153, 61006086). The authors would like to thank the assistance of Pengcheng Xu for the measurement of ATR-FTIR

spectroscopy and the assistance of Shanluo Huang for the data processing.

References

- [1] H.C. Budnikov, G.A. Evtugyn, A.V. Porfireva, *Talanta* 102 (2012) 137–155.
- [2] C. Crean, E. Lahiff, N. Gilmartin, D. Diamond, R. O'Kennedy, *Synth. Met.* 161 (2011) 285–292.
- [3] C. Dhand, M. Das, M. Datta, B.D. Malhotra, *Biosens. Bioelectron.* 26 (2011) 2811–2821.
- [4] R. Gangopadhyay, A.D. Chowdhury, A. De, *Sens. Actuators, B* 171 (2012) 777–785.
- [5] H.A. Zhong, R. Yuan, Y.Q. Chai, W.J. Li, X. Zhong, Y. Zhang, *Talanta* 85 (2011) 104–111.
- [6] D. Shan, Q.F. Shi, D.B. Zhu, H.G. Xue, *Talanta* 72 (2007) 1767–1772.
- [7] Z. Ping, G.E. Nauer, H. Neugebauer, J. Theiner, A. Neckel, *J Chem Soc Faraday T* 93 (1997) 121–129.
- [8] Y. Chen, X.H. Huang, H.S. Shi, B. Mu, Q. Lv, *Asian Pac. J. Cancer Prev.* 13 (2012) 3423–3426.
- [9] P.J. Liao, J.S. Chang, S.D. Chao, H.C. Chang, K.R. Huang, K.C. Wu, T.S. Wung, *Sensors* 10 (2010) 11498–11511.
- [10] S. Sadhasivam, J.C. Chen, S. Savitha, F.H. Lin, Y.Y. Yang, C.H. Lee, *Mater. Sci. Eng., C* 32 (2012) 2073–2078.
- [11] G. Bayramoglu, M.Y. Arica, *Bioprocess Biosyst. Eng.* 35 (2012) 423–431.
- [12] S. Banerjee, D. Konwar, A. Kumar, *Sens. Actuators, B* 171 (2012) 924–931.
- [13] Y. Yan, D.D. Lu, H. Zhou, H.P. Hou, T. Zhang, L.M. Wu, L.K. Cai, *Water Air Soil Pollut.* 223 (2012) 1275–1280.
- [14] V.V.R. Sai, S. Mahajan, A.Q. Contractor, S. Mukherji, *Anal. Chem.* 78 (2006) 8368–8373.
- [15] K.Y. Chumbimuni-Torres, R.E. Coronado, A.M. Mfuh, C. Castro-Guerrero, M.F. Silva, G.R. Negrete, R. Bizios, C.D. Garcia, *RSC Adv.* 1 (2011) 706–714.
- [16] M. Farrell, S. Beaudoin, *Colloid Surf. B* 81 (2010) 468–475.
- [17] B. Huang, H.K. Wu, S. Kim, R.N. Zare, *Lab. Chip* 5 (2005) 1005–1007.
- [18] Q. Xie, Z. Li, C. Deng, M. Liu, Y. Zhang, M. Ma, S. Xia, X. Xiao, D. Yin, S. Yao, *J. Chem. Educ.* 84 (2007) 681–684.
- [19] G. Sauerbrey, *Zeitschrift Fur Physik* 155 (1959) 206–222.
- [20] N. Stasyuk, O. Smutok, G. Gayda, B. Vus, Y. Koval'chuk, M. Gonchar, *Biosens. Bioelectron.* 37 (2012) 46–52.
- [21] K. Radhapyari, P. Kotoky, R. Khan, *Mater. Sci. Eng. C* 33 (2013) 583–587.
- [22] M.J. Shin, J.G. Kim, J.S. Shin, *Int. J. Polym. Mater* 62 (2013) 140–144.
- [23] H.F. Zhang, R.X. Liu, J.B. Zheng, *Synth. Met* 167 (2013) 5–9.
- [24] K. Grennan, A.J. Killard, C.J. Hanson, A.A. Cafolla, M.R. Smyth, *Talanta* 68 (2006) 1591–1600.
- [25] A. Deep, A.L. Sharma, P. Kumar, L.M. Bharadwaj, *Sens. Actuators, B* 171 (2012) 210–215.
- [26] A.D. Chowdhury, A. De, C.R. Chaudhuri, K. Bandyopadhyay, P. Sen, *Sens. Actuators, B* 171 (2012) 916–923.
- [27] F.X. Hu, S.H. Chen, C.Y. Wang, R. Yuan, Y. Xiang, C. Wang, *Biosens. Bioelectron.* 34 (2012) 202–207.
- [28] K. Radhapyari, P. Kotoky, M.R. Das, R. Khan, *Talanta* 111 (2013) 47–53.
- [29] A. Keyhanpour, S.M.S. Mohaghegh, A. Jamshidi, *Biosens. Bioelectron.* 3 (2012) 116.
- [30] E. Lahiff, T. Woods, W. Blau, G.G. Wallace, D. Diamond, *Synth. Met.* 159 (2009) 741–748.
- [31] M. Trchova, T. Sapurina, J. Prokes, J. Stejskal, *Synth. Met.* 135 (2003) 305–306.
- [32] P.C. Rodrigues, M.P. Cantao, P. Janissek, P.C.N. Scarpa, A.L. Mathias, L.P. Ramos, M.A.B. Gomes, *Eur. Polym. J.* 38 (2002) 2213–2217.
- [33] I. Sedenkova, M. Trchova, J. Stejskal, *Polym. Degrad. Stabil.* 93 (2008) 2147–2157.
- [34] M. Trchova, I. Sedenkova, J. Stejskal, *Synth. Met.* 154 (2005) 1–4.
- [35] R. Mazeikiene, V. Tomkute, Z. Kuodis, G. Niaura, A. Malinauskas, *Vib. Spectrosc.* 44 (2007) 201–208.
- [36] J.X. Zhang, C. Liu, G.Q. Shi, *J. Appl. Polym. Sci.* 96 (2005) 732–739.
- [37] G.M. do Nascimento, M.L.A. Temperini, J. Raman Spectrosc. 39 (2008) 772–778.
- [38] M. Jain, S. Annapoorni, *Synth. Met* 160 (2010) 1727–1732.
- [39] L.D. Arsov, W. Plieth, G. Kossmehl, *J. Solid State Electrochem.* 2 (1998) 355–361.
- [40] N.G.R. Mathebe, A. Morrin, E.I. Iwuoha, *Talanta* 64 (2004) 115–120.
- [41] D.D. Borole, U.R. Kapadi, P.P. Mahulikar, D.G. Hundiwale, *J. Mater. Sci.* 42 (2007) 4947–4953.